ISBN: 978-3-95450-168-7 doi:10.18429/JACoW-IPAC2015-TUPJE057

REALISTIC UNDULATORS FOR INTENSE GAMMA-RAY BEAMS AT FUTURE COLLIDERS*

A. Alrashdi[1,2,3†], I. Bailey[1,2], and D. Newton[2,4]
[1]Physics Department, Lancaster University, Lancaster, UK
[2]Cockcroft Institute, Daresbury Science and Innovation Campus, Warrington, UK
[3]King Abdulaziz City for Science and Technology, Riyadh, Kingdom of Saudi Arabia
[4]Department of Physics, University of Liverpool, Liverpool, UK

Abstract

The baseline designs for the ILC and CLIC require the production of an intense flux of gamma rays in their positron sources. In the case of CLIC the gamma rays are produced by a Compton backscattering source, but in this paper we concentrate on undulator-based sources as proposed for the ILC. We present the development of a simulation to generate a magnetic field map based on a Fourier analysis of any measured field map. We have used a field map measured from the ILC helical undulator prototype to calculate the typical distribution of field errors, and used them in our calculations to produce simulated field maps. We show that a loss of gamma ray intensity of ~ 8% could be expected, compared to the ideal case. This leads to a similar drop in positron production which can be compensated for by increasing the undulator length.

INTRODUCTION

In the ILC, to achieve the required gamma-ray flux, a 150 GeV electron beam needs to pass through a long helical undulator (approximately 147 m) with a K of 0.93 and a peak field on-axis of 0.88 T successfully. This undulator nominally contains 84 modules of active length 1.7825 m. Dipole magnets may be used to correct the beam in between the modules to redirect the beam to the central axis. Errors in the undulator field can alter the flux, energy distribution and polarisation of the gamma rays. Below we demonstrate a technique to quantify the effect of these errors.

MAGNETIC FIELD MAP

Ideal Magnetic Field Map

Equations 1 and 2 describe the magnetic field inside an ideal helical undulator,

$$B_x = B_0 \sin \frac{2\pi z}{\lambda_u} \quad (1)$$

$$B_y = B_0 \cos \frac{2\pi z}{\lambda_u} \quad (2)$$

where B_0 is the field strength, z is the distance along the primary axis of the undulator, and λ_u is the period size.

* This research was funded in part by the STFC Cockcroft Institute Core grant no. ST/G008248/1.
† aalrashdi@kacst.edu.sa

Measured Magnetic Field Map

There were two field maps measured from the ILC prototype undulator modules using a Hall probe on-axis [1]. Imperfections in the magnet winding or deformation of the magnet 'former' lead to errors in the field. The magnet prototype field map was manipulated to add tapering for the first 2 and last 2 periods to ensure that the electron will stay close to the centre of the undulator if injected along the centre.

Simulated Magnetic Field Map

In order to produce a simulated magnetic field map based on a measured field map. We introduced errors in the magnetic field strength as well as in the period size over the length of the undulator along the z direction. This is discussed in more detail here [2]. The model used ensures the simulated map will not have a discontinuity. We compared the Discrete Fourier Transforms of the x-projections of the magnetic fields within the undulator for the measured data and simulated data to tune the model.

Our studies suggest that similar trajectories are obtained for particles travelling through the simulated field whether or not the errors in the y projection of the field are calculated independently of those in the x projection of the field. For this work we assumed that the errors in x and y have the same characteristic size and distribution.

TRACKING THE ELECTRON INSIDE THE UNDULATOR

Below we refer to three types of undulator data: ideal, measured, and simulated which we used as input to the HUSR simulation code [3,4]. In the ideal case, an electron will feel an average magnetic field strength of zero and will be transported through the undulator with a total deflection of zero as long as it is injected at an appropriate angle or tapering is used. The electron is injected on axis and the measured and simulated fields are manipulated to add tapering for the first 2 and last 2 periods. Fig 1 shows the position of the electron on the x and y axes. The radius of the helical trajectory has a standard deviation of 8×10^{-12} m reflecting the small numerical uncertainty in the simulation.

ISBN: 978-3-95450-168-7 doi:10.18429/JACoW-IPAC2015-TUPJE057

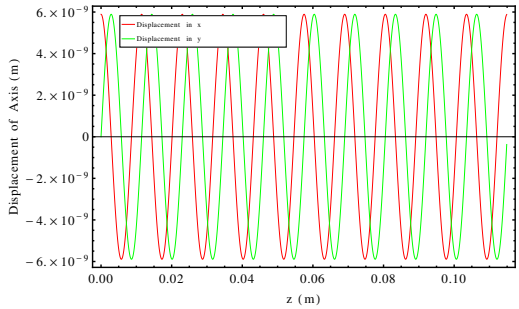

Figure 1: Displacement of a 150 GeV electron through 10 periods of the ILC Ideal helical undulator with a 0.88 T magnetic field strength on axis.

For the measured field map. Fig 2 shows the projection of the electron trajectory in the x and y planes where the maximum deviation in x is -2.5×10^{-6} m and in y is -3.7×10^{-6} m.

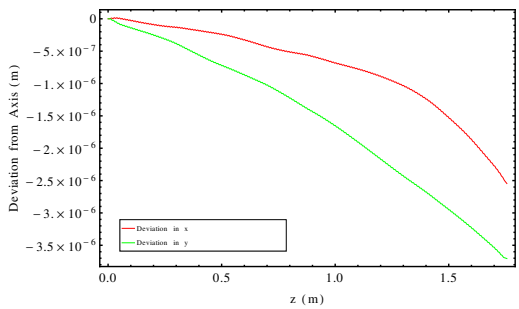

Figure 2: Deviation of a 150 GeV electron through a 1.7825 m long measured undulator with a nominal 0.88 T magnetic field strength on axis. The electron is injected on axis and the measured field is manipulated to add tapering for the first 2 and last 2 periods.

In the simulated field map case to investigate a representative sample of possible trajectories of the electron inside the undulator, we simulated 20 different modules. Fig 3 shows a band representing +/- 1 standard deviation in the x projection of the simulated electron trajectories.

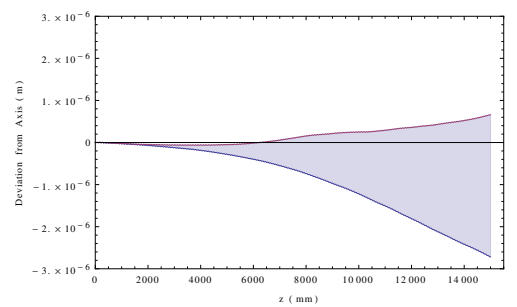

Figure 3: X projection of the trajectories of 150 GeV electrons travelling through simulated 1.7825 m long undulator modules with a nominal magnetic field strength of 0.88 T. The band shows the average trajectory +/- 1 standard deviation as calculated from 20 simulated field maps.

The standard deviation of the trajectories (averaging the results in x and y) is 1.75×10^{-6} m which is similar to the expected beam size given by: $\sigma_x = 3.7 \times 10^{-5}$ m, $\sigma_y = 2.4 \times 10^{-6}$ m, which also has expected divergences given by: $\sigma_{x'} = 0.9 \times 10^{-6}$ rad and $\sigma_{y'} = 0.06 \times 10^{-6}$ rad [5].

SPECTRA FROM FIELD MAPS

In this section, we calculate the energy spectra from the three types of undulators, which were described earlier. Fig. 4 shows the output of the energy spectrum from an ideal undulator system and the measured undulator system as previously described.

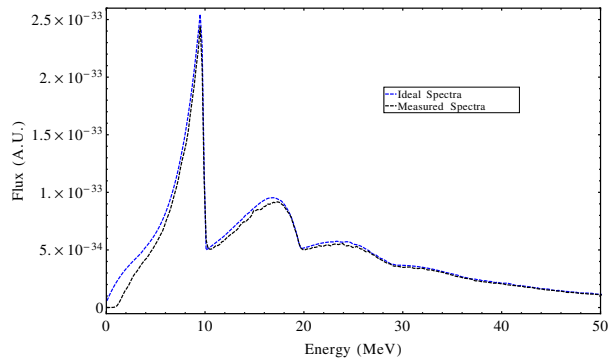

Figure 4: Calculated energy spectrum from tracking a single electron through a 1.7825 m long undulator with a circular aperture with a radius of 0.0045 m at a distance of 500 m from the end of the undulator. The blue dashed line shows the result from an ideal map, and the black dashed line shows the result from the measured map.

Fig. 5 shows the average photon energy spectra with a band representing +/- 1 standard deviation obtained from the 20 models from our simulated field maps. This gives an estimate of the range of the deviation of the spectra which is at a level of 3%.

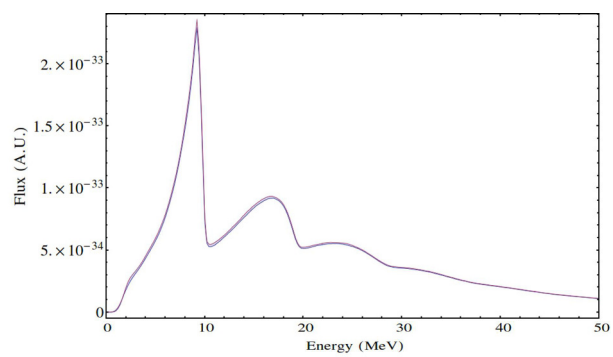

Figure 5: Energy spectrum calculated from the simulated magnetic field maps. The red line represents the average spectrum plus 1 standard deviation and the blue line represents the average spectrum minus 1 standard deviation.

For the measured map, Fig. 6 shows a band representing +/- 1 standard deviation of the spectrum from 5 particles in-

ISBN: 978-3-95450-168-7 doi:10.18429/JACoW-IPAC2015-TUPJE057

jected at random positions in phase space into the measured field map according to the beam sizes specified in the last section.

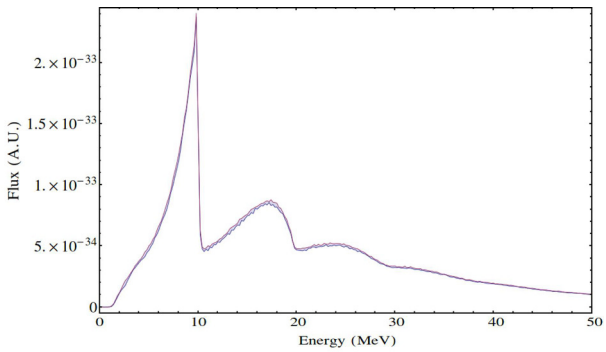

Figure 6: Energy spectrum calculated from the measured field map. The red line represents the average spectrum plus 1 standard deviation and the blue line represents the average spectrum minus 1 standard deviation.

Table 1: Summary table of differences between the ideal and measured energy spectrum using a realistic beam spot size and the energy spectrum from the 20 simulated field maps injected on axis.

Parameters	**Average peak height** (1^{st} *harmonic*) (A.U.)	**Average total flux**
Ideal(no beam spot)	2.532×10^{-33}	$7.775 \times 10^{16}\ \gamma/s$
Ideal (with beam spot)	2.426×10^{-33}	$7.281 \times 10^{16}\ \gamma/s$
Measured (no beam spot)	2.486×10^{-33}	$7.011 \times 10^{16}\ \gamma/s$
Measured (with beam spot)	2.381×10^{-33}	$6.929 \times 10^{16}\ \gamma/s$
Simulated (no beam spot)	2.317×10^{-33}	$7.085 \times 10^{16}\ \gamma/s$

From Table 1, in the case of the measured field map, we can clearly see that the total flux of photons has reduced by ~ 9% overall but the energy flux has only reduced by ~ 1% on the first harmonic compared with the ideal field map when no beam spot is considered. These reductions are due to the errors in the measured field map. In the case of the ideal field map using a realistic beam spot size, we found a reduction by ~ 4% of the peak height on the first harmonic and by ~ 6% for the total flux. The simulated and measured field maps give similar results for the total flux, although the peak of the first harmonic is reduced more on average in the simulated case. Combining both the effects of errors in the magnets and the finite beam size we see a reduction by ~ 6% of the average peak height on the first harmonic and by ~ 11% for the average total flux in the case of the measured field map. Previous studies of earlier designs of the ILC undulator [6] showed that the number of positrons captured and injected into the positron damping ring strongly varies depending upon which harmonic of the undulator spectrum is being considered. For example, the first harmonic contributes only 7% of the total positron yield, whereas the second, third and fourth each contribute around 18%. Using this data along with the modified energy spectra from this work suggests a drop in positron yield of ~ 7% compared to the ideal case.

CONCLUSION

In this paper, we have discussed simulations of errors in the undulator magnetic field of the ILC positron source. We simulated the trajectory of the electron beam inside the measured magnetic field of the ILC helical undulator prototype and developed a tool to generate a simulated field map based on the error from any measured field map.

Based on these simulations, the trajectory of the electron inside the measured field and simulated maps will have maximum deviations from axis of the order of tens of microns. Since the deflection of the beam size is less than the real beam spot size, this deflection should be controllable. The expected reduction in flux from considering the effects of finite beam size and realistic errors in the undulator magnetic field could be compensated for by optimising the beam trajectory through the undulator or if required increasing the undulator length to approximately 160 m.

Carrying out prototype experiments to evaluate the trajectory of the electron and spectrum is expensive. By evaluating the trajectory of the electron and spectrum using a numerical code with a high accuracy and realistic simulated data we hope to turn this initial study into a rigorous investigation.

REFERENCES

[1] Clarke, JA and Bailey, IR and Baynham, E and Bradshaw, TW and Brummitt, A and Bungau, A and Carr, FS and Collomb, NA and Dainton, J and Hartin, AF and others "Construction of a full scale superconducting undulator module for the International Linear Collider Positron Source." The eleventh European Particle Accelerator Conference, EPAC 2008.

[2] Alrashdi, A and Bailey, IR and Newton, D. "Possible uses of gamma-rays at future intense positron sources." (2014): 586-588.

[3] Newton, D. "The rapid calculation of synchrotron radiation output from long undulator systems." Proceedings of IPAC2010, Kyoto, Japan (2010).

[4] Newton, D. "Modeling synchrotron radiation from realistic and ideal long undulator systems." Proceedings of IPAC2010, Kyoto, Japan (2010).

[5] Liu, W and Gai, W and Borland, M and Xiao, A and Kim, Kwang-Je and Sheppard, J and others "Emittance Evolution of the Drive Electron beam in a Helical Undulator for the ILC Positron Source".

[6] Liu, W and Gai, W and Kim K. "Systematic study of the undulator based ilc positron Source: Production and capture." Particle Accelerator Conference, 2007. PAC. IEEE. IEEE, 2007.